Preprints of the 19th World Congress
The International Federation of Automatic Control
Cape Town, South Africa. August 24-29, 2014

Finite-Time Control of an Actuated Orthosis Using Fast Terminal Sliding Mode

T. Madani[▷], B. Daachi[▷] and K. Djouani[◁▷]

[▷] *Laboratoire Images, Signaux et Systèmes Intelligents*
University of Paris East Créteil
122 rue Paul ARMANGOT
94400 Vitry/Seine, France
[◁] *F'SATIE/TUT, Pretoria, South Africa*
(e-mail: tarek.madani@u-pec.fr)

Abstract: This paper deals with the controller of an active orthosis for rehabilitation reasons of the knee joint. The dynamical model of the system, constituted of the shank and the orthosis is complex and is considered as unknown in the conception of the proposed controller. The full security protocol has been carefully applied and we have selected a healthy person for our experiments. The flexion/extension movements used for our experiments are of sinusoidal form and are generally applied by therapeutic doctors. The fast terminal sliding mode technique used in the proposed controller permits a finite time convergence towards zero of the tracking errors both in position and in velocity. The experimental results are satisfactory and prove clearly the effectiveness of the proposed approach. As the wearer used can develop a muscular effort, we have tested the two cases: resistive and assistive effort and we have obtained a good performance in both cases as has been proven in the stability analysis by the the Lyapunov approach.

Keywords: Fast terminal sliding mode control, Finite-time convergence, Exoskeleton

1. INTRODUCTION

Exoskeletons are increasingly developed in the literature and are designed to solve several problems that may be encountered by humans. In fact, nobody is immune to an accident or a pathology causing him a partial/total impairment of its mobility. One can become paraplegic, for instance. Exoskeletons can be used to reduce the degree of dependence regarding to this kind of situations. They are also used in the field of rehabilitation of lower and/or upper limbs. Furthermore, exoskeletons can also be used to improve comfort and assist in various daily tasks (gardening, carry heavy loads, climb stairs, walk longer, etc.). An exoskeleton may either concern a part of the body (arms, knee, pelvis, etc.) or a combination of many parts (both feet with the pelvis for instance). Exoskeletons are widely developed in the literature. In [1], the kinematics, the control and the therapy modes of the arm therapy robot ARMin are presented. The Tokyo University of Agriculture and Technology has designed an exoskeleton to assist its wearer to realize farming work that is considered as tough [2]. In the context of military applications, Hercule has been realized to improve the performances of soldiers [3]. Berkeley University has recently conceived a lower limb exoskeleton named BLEEX that helps its wearer to transport important loads [4]. Finally, one can find in [5] a good state of the art on the exoskeletons and their applications.

In order to allow the exoskeleton to meet the needs of the wearer, it is necessary to develop a suitable control scheme. The complexity of the system dynamics, consisting of the exoskeleton and its wearer, associated with external disturbances, makes conventional controllers inefficient. This complexity has led researchers to several proposals concerning appropriate controllers. Some control schemes are based on a preliminary step of identifying dynamic parameters of the exoskeleton and its wearer. Other approaches are adaptive and are dedicated to generic exoskeletons that can be worn by humans having different morphologies. One example of such controllers is the neural adaptive approach. The universal approximation of neural networks [6] represents one of their advantages. However, neural approaches require a step of offline learning to avoid undesirable behavior of the exoskeleton during the initialization phase. One can also find several works dealing of nonlinear control of exoskeletons [7].

In this paper, we develop and experiment a sliding mode controller for an actuated orthosis. Sliding mode technique is widely applied to solve control problems of nonlinear systems thanks to its robustness for disturbance and model uncertainty [8]. The conventional sliding mode control adopts the Linear Sliding Mode (LSM) surface. In this case, the convergence of system states is only asymptotic. A nonlinear Terminal Sliding Mode (TSM) surface has been designed [9] to ensure the finite-time stability. The Fast Terminal Sliding Mode (FTSM) surface has been introduced [10] to further reduce the finite-settling-time by combining LSM and TSM. We use the FTSM version for our control law synthesis.

The article is organized as follows. In the second section, we describe the exoskeleton used in our experiments and formulate the considered problem. The third section is dedicated to the proposed controller and stability analysis.

The experimental results and their analysis are given in the fourth section. We finish the presentation of the paper with a conclusion and perspectives to this work.

2. ACTIVE ORTHOSIS SYSTEM

The considered system for our experimentations is represented by a human wearing an orthosis composed of two jointed segments, upper and lower. The actuator and the mechanical part are placed on the upper part of the orthosis. The torque generated by the orthosis permits to realize flexion/extension movements of the lower part composed by the shank of the wearer and the lower part of the orthosis. For security reason, the knee joint is constrained by a range of motion between 0 and $\frac{2\pi}{3}$. In Figure 1, we present the actuated knee joint orthosis of LISSI laboratory.

Fig. 1. Actuated knee joint orthosis of LISSI laboratory

2.1 Electrical part

The joint of the orthosis is actuated by a brushless DC motor (BLDC). A power supply and an adequate electrical control system (controller in current mode) are used to provide the regulation for the current in the motor. A mechanical transmission is used to increase the orthosis applied torque.

Assumption 1: The time constant of the current control system is neglectable compared to the mechanical time constant.

According to regulation system characteristics of the BLDC motor and the assumption 1, we can write the following equation:

$$\tau_a = k_m \; i \tag{1}$$

where i is the electrical current of the BLDC motor, τ_a is the applied torque and k_m is a positive constant.

2.2 Mechanical part

The mechanical structure scheme of the considered active orthosis is given by Fig. 2. Let θ the angular position of the knee joint-orthosis in the sagittal plane where 0 corresponds to full knee extension and $\frac{\pi}{2} rad$ represents the resting position.

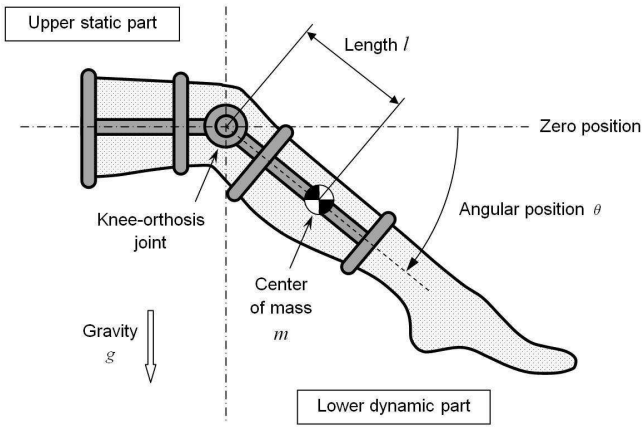

Fig. 2. Position of the joint orthosis

According to the dynamic fundamental principle of solids in rotary motion, it comes:

$$J \; \ddot{\theta} = \sum \tau_i, \tag{2}$$

with $\ddot{\theta}$ is the angular acceleration, J is the total inertia and τ_i are the applied torques to the knee-orthosis joint.

Assumption 2: The set of joint applied torques in the orthosis are formed by: the actuated orthosis torque τ_a, the human knee joint torque τ_k, the gravitational torque τ_g, the resistive viscous friction torque τ_v, the resistive solid friction torque τ_s and the disturbance torque τ_d which includes all other unmodelled dynamics.

From (2) and the assumption 2, the following dynamic model is obtained where $\dot{\theta}$ is the angular velocity of the knee joint-orthosis and g is the gravitational acceleration:

$$J\ddot{\theta} = \tau_a + \tau_k + \tau_d + \underbrace{mgl\cos(\theta)}_{\tau_g} - \underbrace{k_v \; \dot{\theta}}_{\tau_v} - \underbrace{k_s sgn(\dot{\theta})}_{\tau_s}, \tag{3}$$

and k_v is the viscous friction coefficient, k_s is the solid friction coefficient, m is the mass and l is the length.

Assumption 3: The parameters $\{k_m, k_v, k_s, m, l, J\}$ are unknown, bounded and strictly positive constants.

Assumption 4: The torques τ_k and τ_d are unknown and bounded.

2.3 Dynamic model

The following dynamic model of the whole system is obtained by (1) and (3):

$$\ddot{\theta} = f(\theta, \dot{\theta}, t) + \varphi \; u(t) \tag{4}$$

with $u = i$ is the electrical current control input, $\varphi = \frac{k_m}{J}$ and the functions $f(\theta, \dot{\theta}, t) \in \mathbb{R}$ is given by:

$$f(\theta, \dot{\theta}, t) = \frac{1}{J}[mgl \; \cos(\theta) - k_v \; \dot{\theta} - k_s \; sgn(\dot{\theta}) + \tau_k + \tau_d] \tag{5}$$

According to the assumptions 3 and 4, we can write:

$$\begin{cases} \dfrac{1}{\lambda} \leq \varphi \\ |f(\theta, \dot{\theta}, t)| \leq a_0 + a_1|\cos(\theta)| + a_2|\dot{\theta}| \triangleq P(\theta, \dot{\theta}) \end{cases} \tag{6}$$

where a_0, a_1, a_2 and λ are an adequate positive constants.

One can synthesize the control law forcing the states $\{\theta, \dot{\theta}\}$ of a orthosis to follow the desired trajectory by using the fast terminal sliding mode technique.

3. SLIDING MODE CONTROLLER DESIGN

Our objective is to design a sliding mode control law for the actuated orthosis. The controller generates the control signal $u(t)$ ensuring that the real position $\theta(t)$ tracks the desired one $\theta^d(t)$ in finite-time. This can be done in two main steps:

- Select the FTSM switching manifold so that the system in sliding mode guarantees the convergence to the equilibrium point in finite-time (settling time).
- Determine the control law that guarantees the reachability of the sliding manifold and the appearance of the sliding mode in finite-time (reaching time).

Assumption 5: The signals θ and $\dot{\theta}$ can be measured or estimated by embedded sensors.

Assumption 6: The desired position θ^d is twice differentiable with respect to time.

3.1 Stability analysis

In this section, we use the following lemma to prove the finite time stability of the proposed controller. This is the result of the differential inequalities theory [11].

Lemma 1: Let $V(t)$ is a C^1 (continuously differentiable) scalar positive-definite function satisfies the following differential inequality:

$$\dot{V}(t) \leq -\alpha V(t) - \beta V^{\gamma}(t), \quad \forall t \geq t_0, \quad V(t_0) \geq 0, \tag{7}$$

where $\alpha > 0$, $\beta > 0$ and $0 < \gamma < 1$ are constants. Then, for any given t_0, $V(t)$ checks the following inequality:

$$V^{1-\gamma}(t) \leq -\frac{\beta}{\alpha} + \frac{\alpha V^{1-\gamma}(t_0) + \beta}{\alpha} \exp^{-\alpha(1-\gamma)(t-t_0)}, \quad t_0 \leq t < t_1, \tag{8}$$

and:

$$V(t) = 0, \quad \forall t \geq t_1, \tag{9}$$

with the finite time t_1 satisfy:

$$t_1 \leq t_0 + \frac{1}{\alpha(1-\gamma)} \ln \frac{\alpha V^{1-\gamma}(t_0) + \beta}{\beta} \triangleq t^*. \tag{10}$$

Proof: Consider the following differential equation:

$$\dot{X}(t) = -\alpha X(t) - \beta X^{\gamma}(t), \quad \forall t \geq t_0, \quad X(t_0) = V(t_0), \tag{11}$$

where $X(t)$ is a scalar positive-definite function.

It is well known [12] that the solutions $V(t)$ of (7) and $X(t)$ of (11) satisfies $V(t) \leq X(t)$ for $t_0 \leq t < t_1$. Therefore we can write the following inequality:

$$V^{1-\gamma}(t) \leq X^{1-\gamma}(t), \quad t_0 \leq t < t_1. \tag{12}$$

Although the differential equation (11) does not satisfy the global *Lipschitz* condition, we proceed now to found its unique solution. This equation can be rearranged as:

$$X^{-\gamma}\dot{X} + \alpha X^{1-\gamma} = -\beta. \tag{13}$$

By introducing the following variable change:

$$Y = X^{1-\gamma}, \tag{14}$$

its yields:

$$\dot{Y} + AY = B, \tag{15}$$

where:

$$A = +\alpha(1-\gamma), \; B = -\beta(1-\gamma). \tag{16}$$

The general solution of a first-order linear differential equation (15) is:

$$Y(t) = \exp^{-\int_{t_0}^{t} A dt} \left\{ \int_{t_0}^{t} B \exp^{\int_{t_0}^{t} A dt} dt + C \right\}, \tag{17}$$

with $C = Y(t_0)$.Since $Y(t)$ is a positive-definite function then:

$$Y(t) = \begin{cases} \dfrac{B}{A} + \dfrac{AC - B}{A} \exp^{-A(t-t_0)} & \text{if } t_0 \leq t < t^*, \\ 0 & \text{if } t \geq t^*, \end{cases} \tag{18}$$

with:

$$t^* = t_0 + \frac{1}{A} \ln \frac{AC - B}{-B}. \tag{19}$$

It easy to verify that the above expression of t^* is the same one given in (10).

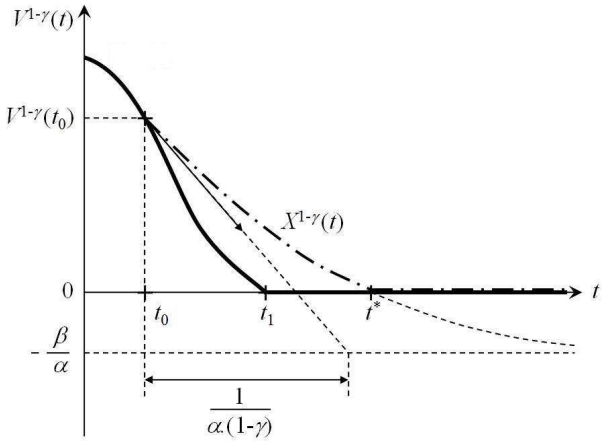

Fig. 3. Finite-time convergence

By using (16), (18) and the change of variable (14), the following expressions can be written:

$$X^{1-\gamma}(t) = -\frac{\beta}{\alpha} + \frac{\alpha X^{1-\gamma}(t_0) + \beta}{\alpha} \exp^{-\alpha(1-\gamma)(t-t_0)}, \quad t_0 \leq t < t^*, \tag{20}$$

and:

$$X^{1-\gamma}(t) = 0, \quad \forall t \geq t^*. \tag{21}$$

Finally, by using the property (12) we can write (8) and (9).The Fig. 3 shows a graphical representation of the considered finite-time convergence.

3.2 Switching law selection

Consider the following FTSM switching law [10]:

$$s \triangleq \dot{e} + \alpha_s e + \beta_s |e|^{\gamma_s} sgn(e), \tag{22}$$

where $\alpha_s > 0$, $\beta_s > 0$, $0 < \gamma_s < 1$ are constants and e is the tracking error such as:

$$e \triangleq \theta^d - \theta.$$

The used sliding manifold guarantees the finite-time convergence of the error e via the following dynamic equation:

$$\dot{e} = -\alpha_s e - \beta_s |e|^{\gamma_s} sgn(e). \quad (23)$$

Let t_r be the reaching time to the sliding manifold and assuming that sliding mode is maintained after this time i.e.:

$$s(t) = 0, \quad \forall t \geq t_r \quad (24)$$

The finite-time convergence of the sliding mode can be proved by the following *Lyapunov* function for the sliding phase:

$$V_s(t) = \frac{1}{2}e^2(t), \quad \forall t \geq t_r, \quad V_s(t_r) \geq 0. \quad (25)$$

Its time derivative is:

$$\begin{aligned} \dot{V}_s &= e\dot{e} \\ &= e[-\alpha_s e - \beta_s |e|^{\gamma_s} sgn(e)] \\ &= -\alpha_s e^2 - \beta_s |e|^{1+\gamma_s}. \end{aligned} \quad (26)$$

The following equivalent equation is obtained from (26) by replacing e^2 and $|e|$ by $2V_s$ and $\sqrt{2V_s}$ respectively:

$$\dot{V}_s = -2\alpha_s V_s - 2^{\frac{1+\gamma_s}{2}} \beta_s V_s^{\frac{1+\gamma_s}{2}}. \quad (27)$$

According to the Lemma 1, since (27) and the accuracy of the following inequalities:

$$2\alpha_s > 0, \ 2^{\frac{1+\gamma_s}{2}} \beta_s > 0, \ \frac{1}{2} < \frac{1+\gamma_s}{2} < 1, \quad (28)$$

then we can write $e(t) = 0$ for $t \geq t_s$ with t_s is the settling time given by:

$$\begin{aligned} t_s &= t_r + \frac{1}{2\alpha_s(1-\frac{1+\gamma_s}{2})} \ln \frac{2\alpha_s V_r^{1-\frac{1+\gamma_s}{2}}(t_r) + 2^{\frac{1+\gamma_s}{2}}\beta_s}{2^{\frac{1+\gamma_s}{2}}\beta_s} \\ &= t_r + \frac{1}{\alpha_s(1-\gamma_s)} \ln \frac{\alpha_s |e(t_r)|^{1-\gamma_s} + \beta_s}{\beta_s}. \end{aligned} \quad (29)$$

The elapsed time t_r will be specified in the next section.

3.3 Sliding mode control

The main objective is to generate control law $u(t)$ to achieve and maintain the sliding mode $s = 0$. Thus, the output θ should track the desired trajectory θ^d in finite time, where the trajectory can be an arbitrary function of time.

We propose the following control law:

$$\begin{aligned} u = \lambda\{\alpha_r s + sgn(s)[\, \beta_r |s|^{\gamma_r} + P(\theta, \dot{\theta}) + |\ddot{\theta}^d| \\ +(\alpha_s + \beta_s \Phi_{\gamma_s}(e))|\dot{e}|\ ]\ \} \end{aligned} \quad (30)$$

with $\alpha_r > 0$, $\beta_r > 0$, $0 < \gamma_r < 1$ are constants and:

$$\Phi_{\gamma_s}(e) = \begin{cases} \gamma_s |e|^{\gamma_s - 1} & \text{if } e \neq 0 \\ 0 & \text{if } e = 0 \end{cases} \quad (31)$$

Theorem 1: Under the controller (30), the trajectory of the closed-loop system (4) can be driven onto the sliding surface $s(t) = 0$ in a finite time.

Proof: Consider the following *Lyapunov* function for the reaching phase:

$$V_r(t) = \frac{1}{2}s^2(t), \quad \forall t \geq 0, \quad V_r(0) \geq 0. \quad (32)$$

The derivative of the switching law (22) is given by:

$$\begin{aligned} \dot{s} &= \ddot{e} + \alpha_s \dot{e} + \beta_s \gamma_s |e|^{\gamma_s - 1} \dot{e} \\ &= \ddot{\theta}^d - \ddot{\theta} + (\alpha_s + \beta_s \gamma_s |e|^{\gamma_s - 1})\dot{e}. \end{aligned} \quad (33)$$

It can be seen from (33) that $\dot{s}$ contains the term $|e|^{\gamma_s - 1}\dot{e}$ which has negative power $(\gamma_s - 1)$. Therefore, the singularity may occur if $\{e = 0 \text{ and } \dot{e} \neq 0\}$. In fact, this situation can be done just a passing moment but it can never be maintained. Furthermore, this configuration does not contain the equilibrium point $e = \dot{e} = 0$. So let consider the complementary case $\{e \neq 0 \text{ or } \dot{e} = 0\}$ in the following of the proof.

By putting (4) in (33) yields:

$$\dot{s} = \ddot{\theta}^d + (\alpha_s + \beta_s \gamma_s |e|^{\gamma_s - 1})\dot{e} - f(\theta, \dot{\theta}, t) - \varphi\, u. \quad (34)$$

Replacing the control law (30) in (34), one can obtain the following equality:

$$\begin{aligned} \dot{s} = -f(\theta, \dot{\theta}, t) + \ddot{\theta}^d + (\alpha_s + \beta_s \gamma_s |e|^{\gamma_s - 1})\dot{e} \\ - \lambda\varphi\{\alpha_r s + sgn(s)[\, \beta_r |s|^{\gamma_r} + P(\theta, \dot{\theta}) + |\ddot{\theta}^d| \\ +(\alpha_s + \beta_s \gamma_s |e|^{\gamma_s - 1})\, |\dot{e}|\ ]\ \} \end{aligned} \quad (35)$$

By (35) and (36), the following time derivatives of V_r is come:

$$\begin{aligned} \dot{V}_r &= s\dot{s} \\ &= s\{-f(\theta, \dot{\theta}, t) + \ddot{\theta}^d + (\alpha_s + \beta_s \gamma_s |e|^{\gamma_s - 1})\dot{e}\} \\ &\quad -\lambda\varphi\, |s|\, \{P(\theta, \dot{\theta}) + |\ddot{\theta}^d| + (\alpha_s + \beta_s \gamma_s |e|^{\gamma_s - 1})\, |\dot{e}|\} \\ &\quad -\lambda\varphi s\{\alpha_r s + \beta_r |s|^{\gamma_r} sgn(s)\}. \end{aligned} \quad (36)$$

From (6), it is easy to verify that $\lambda\varphi \geq 1$ and:

$$\begin{aligned} s\left\{-f(\theta, \dot{\theta}, t) + \ddot{\theta}^d + (\alpha_s + \beta_s \gamma_s |e|^{\gamma_s - 1})\dot{e}\right\} \\ \leq \\ \lambda\varphi\, |s|\left\{P(\theta, \dot{\theta}) + |\ddot{\theta}^d| + (\alpha_s + \beta_s \gamma_s |e|^{\gamma_s - 1})\, |\dot{e}|\right\} \end{aligned} \quad (37)$$

Therefor $\dot{V}_r$ satisfies:

$$\dot{V}_r \leq -\lambda\varphi\alpha_r s^2 - \lambda\varphi\beta_r |s|^{\gamma_r + 1}. \quad (38)$$

The following equivalent inequality is obtained from (38) by replacing s^2 and $|s|$ by $2V_r$ and $\sqrt{2V_r}$ respectively:

$$\dot{V}_r \leq -2\lambda\varphi\alpha_r V_r - 2^{\frac{\gamma_r + 1}{2}} \lambda\varphi\beta_r V_r^{\frac{\gamma_r + 1}{2}}. \quad (39)$$

By Lemma 1, since (39) and the coherence of following conditions:

$$2\lambda\varphi\alpha_r > 0, \ 2^{\frac{\gamma_r + 1}{2}} \lambda\varphi\beta_r > 0, \ \frac{1}{2} < \frac{\gamma_r + 1}{2} < 1, \quad (40)$$

then the sliding manifold is achieved at the reaching time t_r given by:

$$\begin{aligned} t_r &\leq \frac{1}{2\lambda\varphi\alpha_r(1-\frac{1+\gamma_r}{2})} \\ &\quad \times \ln \frac{2\lambda\varphi\alpha_r V_r^{1-\frac{1+\gamma_r}{2}}(0) + 2^{\frac{\gamma_r + 1}{2}}\lambda\varphi\beta_r}{2^{\frac{\gamma_r + 1}{2}}\lambda\varphi\beta_r} \\ &\leq \frac{1}{\alpha_r(1-\gamma_r)} \ln \frac{\alpha_r |s(0)|^{1-\gamma_r} + \beta_r}{\beta_r}. \end{aligned} \quad (41)$$

This implies that the FTSM is achieved and (24) is satisfied.

3.4 Chattering elimination

It is well known that sliding mode control signal is discontinuous in nature on the switching manifold, which induces a chattering phenomenon [8]. The latter appears as a very high-frequency oscillation about the sliding surface and may also act as a source that excites the unmodelled high-frequency dynamics of the actuated orthosis. To avoid the effect of this phenomenon, the sign function $sgn(s)$ can be approximated by the saturation function $sat_\delta(s)$ as follows:

$$sat_\delta(s) = \begin{cases} sgn(s) & \text{if } |s| > \delta \\ s/\delta & \text{if } |s| \leq \delta \end{cases} \quad (42)$$

where $\delta > 0$ is a small positive constant.

4. EXPERIMENT RESULTS

In order to validate the proposed strategy, we implemented the control law on a PC equipped with a dSpace DS1103 PPC real-time controller card, using Matlab/Simulink and dSpace Control Desk software. The purpose of the test is to ensure the good performance of the actuated orthosis to help therapists apply their rehabilitation program in good conditions. The experiment considers a healthy subject being 40 years old, weighing $73kg$ and measuring $1.78m$. Fig. 4 shows our experimental setup.

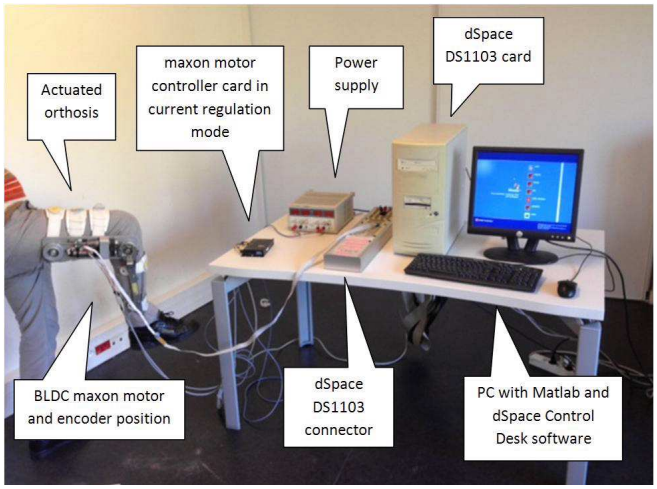

Fig. 4. Experimental setup

Table 1 gives the physical characteristics of the used orthosis.

Parameter	Value	Unit
J	0.4	$Kg.m^2$
k_v	1	$N.m.s.rad^{-1}$
k_s	0.6	$N.m$
$m.g.l$	5	$N.m$

Table 1. Physical parameters of the orthosis

The sampling time has been fixed to 10^{-3} sec. The real position is measured by incremental encoder. A low pass first order filter is used to reduce measurement noise of the angular position. The controller parameters are fixed at: $\alpha_s = 0.1$, $\beta_s = 0.1$, $\gamma_s = 0.5$, $\alpha_r = 10$, $\beta_r = 1$, $\gamma_r = 0.5$, $a_0 = 2$, $a_1 = 1.5$, $a_2 = 0.5$, $\lambda = 2$, $\delta = 0.1$. The considered desired trajectory is of the following form:

$$\theta^d(t) = 1.5 + 0.5\cos(t - 1.1) \quad (43)$$

The initial conditions are:

$$\theta(0) = 1.46\ rad,\ \dot{\theta}(0) = 0\ rad/\sec. \quad (44)$$

By (43) and (44), the tracking errors and the switching law at $t = 0$ sec are:

$$\left.\begin{array}{l} e(0) = 0.26\ rad \\ \dot{e}(0) = 0.45\ rad/\sec \end{array}\right\} \Longrightarrow s(0) = 0.52 \quad (45)$$

This allows us to calculate the theoretical reaching and settling time inequalities based on (41) and (29):

$$t_r \leq 0.42\,\text{sec},\ t_s \leq 8.04\,\text{sec}, \quad (46)$$

with the inequality of the settling time t_s is computed by considering $|e(t_r)| \leq |e(0)|$.

In order to evaluate the robustness performances of the proposed approach, the subject exerts a resistive $\{\tau_k.\tau_a < 0\}$ and the assistive $\{\tau_k.\tau_a > 0\}$ muscular effort in harmony with the orthosis movement.

Remark: The magnitudes of the disturbance torques applied by the subject are not measurable. The only available information is the torque direction. This is sufficient to know the resistive or assistive nature of the effort.

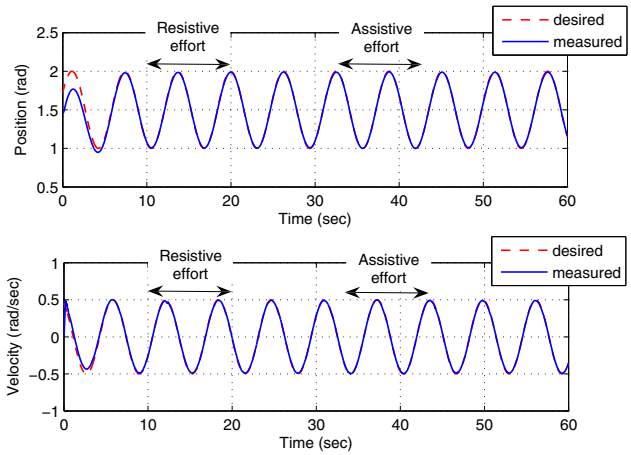

Fig. 5. Measured and desired trajectories

The figures 5 shows the measured and the desired position and velocity trajectories. From these figures, we see the good tracking of the trajectories despite the disturbances applied by the subject. The measured trajectories faithfully follow the desired ones even with the resistive or assistive human efforts.

To show the reaching and settling times, we present in Fig. 6 the evolution of the switching law s and tracking error e during the beginning of the experiment. We notice that with a consideration of the convergence at $\pm 5\%$, the reaching time $t_r = 0.2$ sec and the settling time $t_s = 7.5$ sec which are consistent with the theoretical inequalities (46).

Fig. 7 presents the tracking error trajectory in the phase plane $\{e, \dot{e}\}$. We observe the reaching and the sliding phases of the close loop system. The tracking error is quite similar to that imposed by the sliding surface in the sliding phase. The difference between them is justified by the approximation of the sliding mode system by the saturation function (42).

The real current control signal u is shown in Fig. 8. We notice the good electrical control in both cases with the

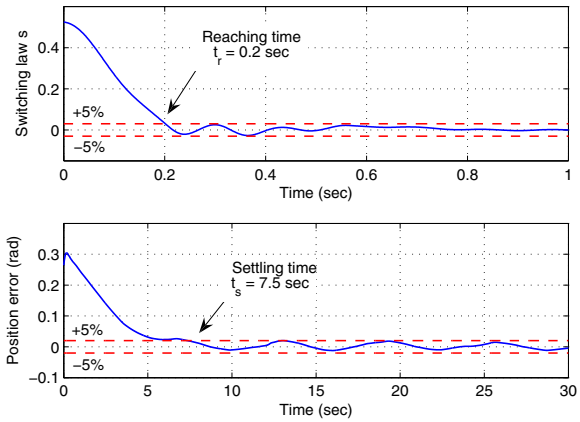

Fig. 6. Reaching and settling times

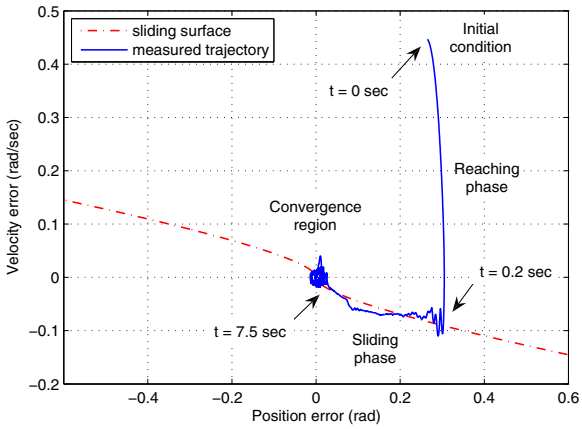

Fig. 7. Reaching and sliding phases in the phase plane

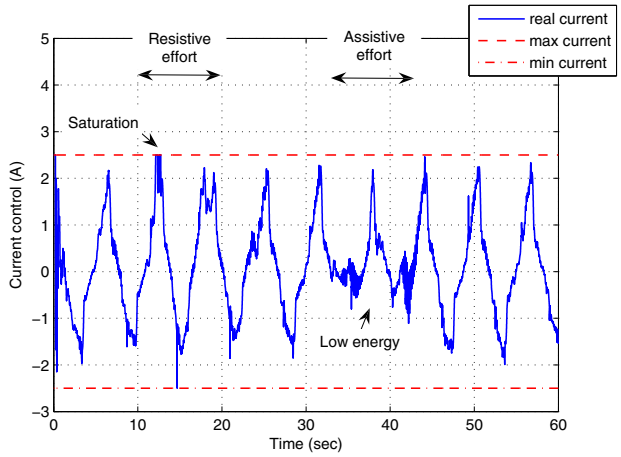

Fig. 8. Control input

considered disturbances. The control energy increases if the disturbance torque is resistive and decreases if otherwise. The control is correct and feasible in practice. The high excitation of the power electrical system is discarded thanks to the chattering phenomenon elimination.

5. CONCLUSION

An efficient controller that ensures convergence towards the performances desired by the wearer of the orthosis, has been developed. Two steps summarize the proposed approach. The first step consists of selecting the FTSM switching manifold so that the system in sliding mode guarantees the convergence to the equilibrium point in finite-time. Then we determine the control law that guarantees the reachability of the sliding manifold and the appearance of the sliding mode in finite-time. From theoretical point of view, the system controlled by our approach, is stable according to the Lyapunov formalism. Concerning the experiment results, we note that all applied flexion/extension movements have been realized smoothly regarding the actuator and the wearer felt at ease. In other hand, the proposed controller responded correctly to resistive and assistive muscular efforts applied by the wearer. For future works, along with the heavy security protocol, we plan to apply the proposition in real case of rehabilitation of the knee joint.

REFERENCES

[1] T. Nef, M. Mihelj and R. Riener, "ARMin: a robot for patient cooperative arm therapy", Medical & Biological Engineering & Computing Vol. 45, pp. 887–900, 2007.

[2] S. Toyama and G. Yamamoto, "Development of Wearable-Agri-Robot ˜mechanism for agricultural work", IEEE IROS, pp. 5801-5806, 2009.

[3] http://www.army-technology.com/features/featurefrench-hercule-robotic-exoskeleton

[4] A. B. Zoss, H. Kazerooni, and A. Chu, "Biomechanical design of the Berkeley lower extremity exoskeleton (BLEEX)", IEEE/ASME Transactions on Mechatronics, Vol. 11, No. 2, pp. 128-138, 2006.

[5] R. Jiménez-Fabián and O. Verlinden, "Review of control algorithms for robotic ankle systems in lower-limb orthoses, prostheses, and exoskeletons", Medical Engineering & Physics, Vol. 34, pp. 397–408, 2012.

[6] M. Gomes, G. Silveira and A. Siqueira, "Gait Pattern Adaptation for an Active Lower-Limb Orthosis Based on Neural Networks", Advanced Robotics, Vol. 25, No. 15, pp. 1903-1925, 2011.

[7] S. Jezernik, R. G. V. Wassink and T. Keller, "Sliding mode closed-loop control of FES: controlling the shank movement", IEEE Transactions on Biomedical Engineering, Vol. 51, No. 2, pp. 263–72, 2004.

[8] V. I. Utkin, "Sliding Modes in Control Optimization" Berlin, Heidelberg: Springer-Verlag, 1992.

[9] S. T. Venkataraman and S. Gulati, "Control of nonlinear systems using terminal sliding modes". Proc. Amer. Control Conf, pp. 891-893, 1989.

[10] X. H. Yu and Z. H. Man, "Fast terminal sliding-mode control design for nonlinear dynamical systems", Fundamental Theory and Applications, IEEE Trans. on Circuits and Systems, vol.49, no.2, pp.261-264, 2002.

[11] J. K. Hale, "Ordinary Deferential Equations", Krieger, Huntington, 1969.

[12] Y. Tang, "Terminal Sliding Mode Control for Rigid Robots", Automatica, Vol. 34. No. 1, pp. 51-56, 1998.